Comparative studies of Si-doped n-type MOVPE GaAs on Ge and GaAs substrates

M.K. Hudait [1,a,b], P. Modak [b], S. Hardikar [b], K.S.R.K. Rao [c], S.B. Krupanidhi [a,*]

[a] *Materials Research Centre, Indian Institute of Science, Bangalore-560 012, India*
[b] *Central Research Laboratory, Bharat Electronics, Bangalore-560 013, India*
[c] *Department of Physics, Indian Institute of Science, Bangalore-560 012, India*

Abstract

Comparative studies of silicon (Si) incorporation in GaAs on both polar GaAs and nonpolar Ge substrates by low temperature photoluminescence (LTPL) spectroscopy were carried out. The PL spectrum shifts towards higher energy with growth temperature, arsine (AsH_3) and trimethylgallium (TMGa) mole fractions on Ge substrates; whereas the PL spectrum shifts towards higher energy with growth temperature and shifts to lower energy with AsH_3 and TMGa mole fractions on GaAs substrates. The shift in PL peak energy towards the higher energy is due to the increase in electron concentration The full width at half maximum (FWHM) increases with increasing growth temperature, AsH_3 and TMGa mole fractions on Ge substrates. But the FWHM increases with increasing growth temperature and decreases with increasing AsH_3 and TMGa mole fractions on GaAs substrates. A vacancy control model may explain the PL peak shift towards higher energy with increasing AsH_3 mole fraction on Ge substrates and with increasing TMGa mole fraction on GaAs substrates. The experimental results of the studies of the effect of TMGa mole fraction variation on zinc (Zn)-doped GaAs on both GaAs and Ge substrates were presented for better understanding of the growth process. © 1998 Elsevier Science S.A. All rights reserved.

Keywords: Gallium arsenide; Optical properties; Germanium; Solar cell

1. Introduction

GaAs/Ge epitaxial heterostructures (HSs) have received a lot of attention as starting materials for the fabrication of photovoltaic devices [1–6] and in electronic and optoelectronic devices [7–9]. The high hole mobility of Ge, as well as its narrow band-gap makes the GaAs/Ge heterojunction suitable for the fabrication of p-channel field-effect transistors, phototransistors and quantum confinement devices [9,10]. Owing to its high mechanical strength, Ge is an optimized substrate material in terms of the power-to-weight ratio for high efficiency GaAs/Ge solar cells [11,12]. As large area, minority carrier devices, III–V/Ge cells are extremely sensitive to defects. Thus, elimination of antiphase domains (APDs) that are characteristic features of the polar epitaxy-on-nonpolar substrate. The suppression of large-scale interdiffusion across the GaAs/Ge heterointerface remains a key challenge for increased yield, reliability and performance.

The Si-doped GaAs on Ge, i.e. polar-on-nonpolar, and on GaAs, i.e. polar-on-polar substrates, by metal organic vapor phase epitaxy (MOVPE) is an important issue of the optical and electrical properties, not only from a fundamental understanding but also for the device applications, such as the buffer and base layer of solar cells. The deposition of GaAs on Ge basically poses the same problems, similar to those observed in the epitaxial growth of layers with different lattice constants (e.g. InGaAs on InP) [11]. However, in this case, there are two other problems that need to be tackled, i.e. the creation of APDs between the polar GaAs and the nonpolar Ge [13–21], and the interdiffusion of Ga, As and Ge across the semiconductor interface [15,22–24]. To avoid the formation of APDs, harmful to solar cell performance as they reduce the short-circuit current, misoriented substrates were used.

* Corresponding author. Tel.: +91 80 3311330; fax: +91 80 3341683; e-mail: sbk@mrc.iisc.ernet.in
[1] E-mail: mantu@mrc.iisc.ernet.in

M. F. of SiH_4 = 5.18x10^{-7}
M. F. of TMGa = 1.78x10^{-4}
M. F. of AsH_3 = 1.57x10^{-2}
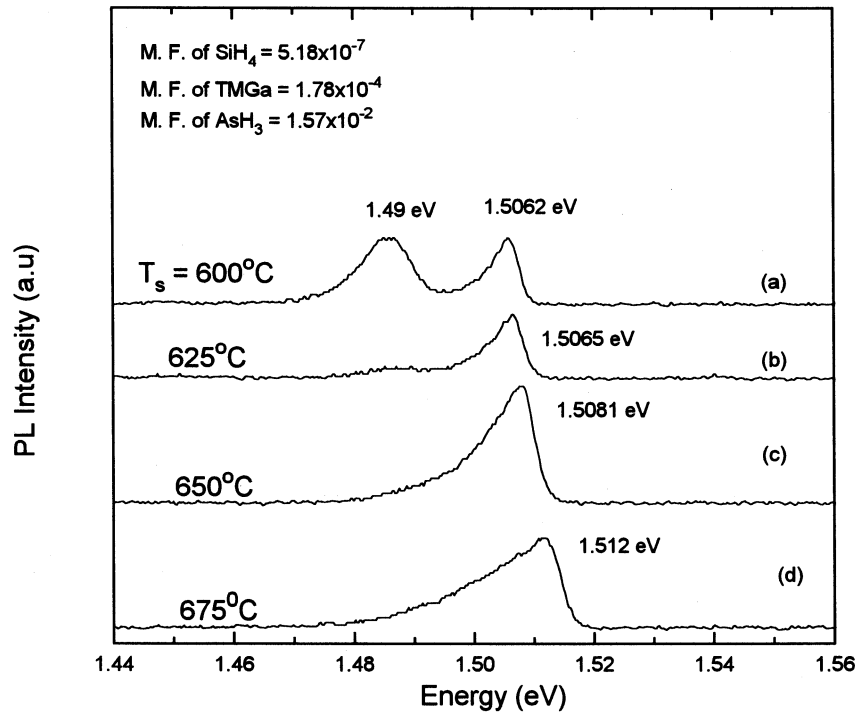
Fig. 1. PL spectra of Si-doped GaAs epilayers grown under various growth temperature on Ge substrates. The corresponding electron concentrations are: (a) 8×10^{16} cm^{-3}, (b) 1.7×10^{17} cm^{-3}, (c) 2.3×10^{17} cm^{-3}, (d) 5.7×10^{17} cm^{-3}.

A further optimization of the GaAs growth conditions on Ge needed for the reduction of the element interdiffusion across the GaAs/Ge interface. The main problem is to reduce the Ga diffusion into the Ge substrate to avoid the formation of an unwanted p-n junction that could affect the performance of the GaAs/Ge solar cells [6].

With the advancement of molecular beam epitaxy (MBE), Ge was successfully grown on GaAs [25]. The reverse (GaAs/Ge), although it had device applications [24,26,27], proved much more difficult. Attempts to grow Ge/GaAs superlattices by MBE have shown that GaAs grows in islands on (100) Ge, resulting in APD [28]. GaAs grown on (100) Ge by vapor phase epitaxy (VPE) also shows APDs [18]. A detailed study of the optimal growth conditions for APD-free GaAs growth on Ge by metal organic chemical vapor deposition (MOCVD) has recently been reported by Li et al. [13,14]. They found that a combination of a large substrate off-cut toward an in-plane ⟨110⟩ coupled with a high substrate temperature ($\approx 650°$C or higher), relatively low growth rate (below 2 μm h^{-1}), and a high As/Ga ratio ($\approx 60:1$) are the requirements for APD-free MOCVD GaAs [14]. No electrical doping measurement was done on these films, but evidence for massive Ge outdiffusion into GaAs grown on Ge by MOCVD at high growth temperatures and low growth rates has been previously reported [15]; with the Ge outdiffusion being sufficient to produce a Burstein–Moss (band-filling) shift in the room temperature photolumines-

cence (PL) spectra of thick layers, and to affect the X-ray rocking curves of thin layers. Since Ge diffusion into GaAs occurs via Ga vacancies [15] and the Ga vacancy population will increase with increasing V/III ratio and decreasing growth rate (i.e. lower Ga flow), it appears that the conditions for APD suppression identified by Li et al. [13,14] are likely to result in significant Ge outdiffusion, and further work is required to identify MOCVD growth conditions that simultaneously produce APD suppression and chemically sharp interfaces. The best MOCVD material [13,14] has been grown using initial arsine exposure. In contrast, it has been reported that when using gas source MBE (cracked arsine and a Ga effusion furnace) a Ga prelayer is required to obtain good GaAs material on a thick Ge film grown on a Si substrate [29–32]. Recently, Timò et al. [33] used the Ge substrates whose orientation was (100) 9° off towards [111] for AlGaAs/GaAs/Ge solar cells by LP-MOVPE. Few reports [15,33,34] on Si-doped GaAs on Ge are available for the indirect information on the interdiffusion phenomena by PL investigations. Therefore, the selection of off-oriented Ge substrates for the deposition of GaAs epitaxial layers by LP-MOVPE is still controversial. There is no unique rule for optimal off-set in orientation of Ge substrate could be used to suppress the APDs during the MOVPE growth of GaAs.

The aim of this work is the detailed study of the effect of growth temperature, V/III ratio, and growth rate on Si-doped GaAs on both GaAs and Ge sub-
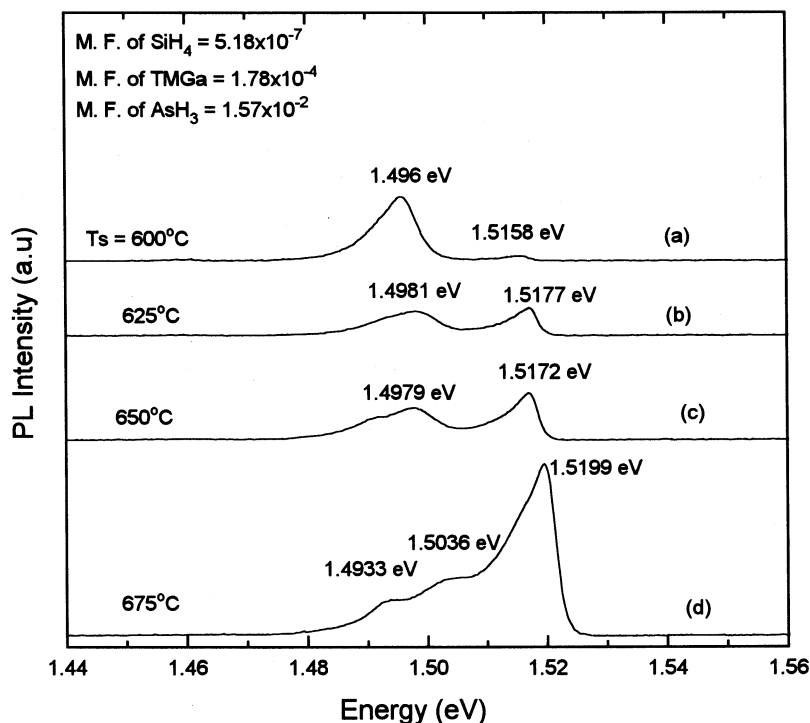
Fig. 2. PL spectra of Si-doped GaAs epilayers grown under various growth temperature on GaAs substrates. The corresponding electron concentrations are: (a) 1.3×10^{17} cm^{-3}, (b) 2.45×10^{17} cm^{-3}, (c) 3.64×10^{17} cm^{-3}, (d) 6.65×10^{17} cm^{-3}.

strates by PL spectroscopy for solar cell applications. The study leads to the establishment of optimum growth conditions which reproducibly generate GaAs films on Ge that are assumed to be APD-free, and which limit outdiffused Ge concentration of the GaAs/Ge heterointerface. The electron concentration increases with increasing growth temperatures, AsH$_3$ and TMGa mole fractions on Ge substrates, whereas the electron concentration increases with increasing growth temperature and decreases with increasing AsH$_3$ and TMGa mole fractions on GaAs substrates. A vacancy control model was found to be suitable to explain the results of our AsH$_3$ variation on Ge substrate and TMGa variation on GaAs substrates. Finally, we have grown the Zn-doped GaAs on both GaAs and Ge substrates for better understanding of the growth process on Ge substrate.

2. Experimental details

The Si-doped n-type and p-type GaAs were grown in each run in a low pressure horizontal MOVPE reactor on Sb doped n$^+$-Ge (100) 6° off orientation towards the [110] direction, n$^+$-GaAs (100) and Cr-doped semi-insulating GaAs (100) substrates, with an offset of 2° towards the [110] direction. The source materials were TMGa, (100%) arsine (AsH$_3$), (104 ppm), silane (SiH$_4$) as an n-type dopant, dimethylzinc (DMZn) as a p-type

dopant and palladium-purified H$_2$ as a carrier gas. During the growth, the pressure inside the reactor was kept at 100 torr and the growth temperature was varied from 600 to 675°C. TMGa and AsH$_3$ flow rates were varied from 5 to 20 SCCM and 30 to 100 SCCM, respectively. The total flow rate was ≈ 2 SLPM. Prior to the growth, the Ge substrates were degreased with organic solvents, then etched in HF:H$_2$O$_2$:H$_2$O (1:1:30) for 15 s according to the specification given by Ge substrate supplier, Laser Diode, USA. The details of the growth procedure may be found elsewhere [35].

PL measurements were carried out using a MIDAC Fourier Transform PL (FTPL) system at a temperature of 4.2 K and 100 mW laser power. An argon ion laser operating at a wavelength of 5145 A° was used as a source of excitation. The exposed area was ≈ 3 mm^2. PL signals were detected by a LN$_2$-cooled Ge-photodetector whose operating range is 0.75–1.9 eV, while resolution was kept at ≈ 0.5 meV. The doping concentrations were determined by using Bio-Rad electrochemical capacitance voltage (ECV) polaron profiler.

3. Results and discussion

3.1. Effect of growth temperature on photoluminescence

Fig. 1 shows the 4.2 K PL spectra obtained from the Si-doped GaAs epilayers on Ge substrate grown at
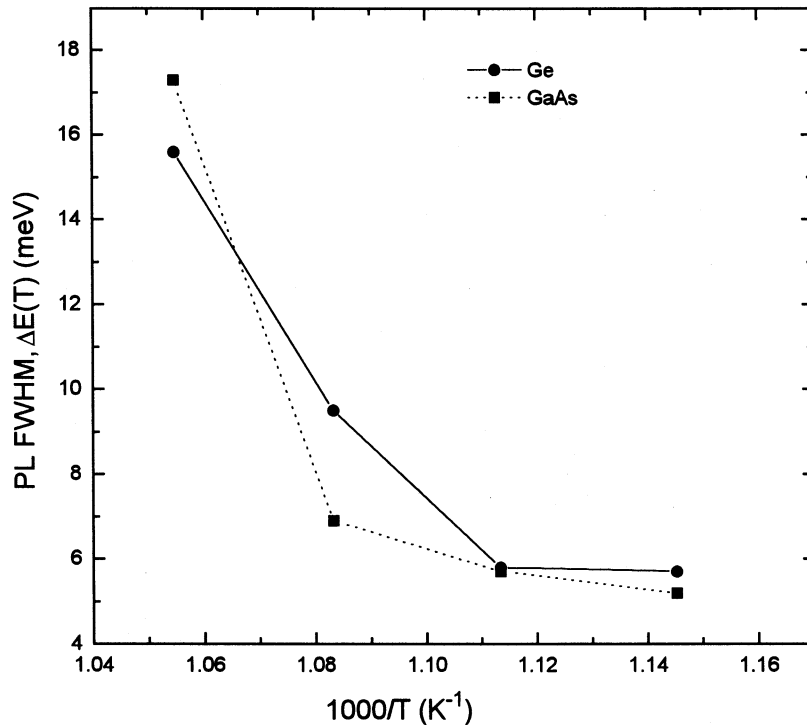
Fig. 3. FWHM of 4.2 K PL vs. growth temperatures.

different growth temperatures. The curves were intentionally offset along the y-axis with respect to each other for better clarity. The same procedure was used for all other PL spectra in this paper. When the electron concentration is relatively low, the spectrum becomes symmetric, while higher electron concentrations lead to asymmetric spectra. The Si doping broadens the excitonic emission until it becomes a wide band-to-band (B–B) luminescence. The peak at 1.49 eV has been attributed to band-to-acceptor (B–A) transitions involving residual carbon (C) impurities present in MOVPE GaAs [36]. The energy separation between the B–A peak and the B–B peak (band gap of GaAs at 4.2 K is 1.5194 eV) is consistent with typical acceptor ionization energies such as that of C ($E_a \approx 26.4$ meV) [37], which is a p-type dopant in MOVPE. The B–A transitions were observed at growth temperatures $\leq$ 600°C and decreases with increasing growth temperatures. From the Fig. 1 it can be seen that beyond the growth temperature of 625°C in our case, only one broad emission band was found, and the peak maximum of the dominant emission E_{max} shifted monotonically towards higher energy with increasing free carrier concentration. According to Burstein and Moss [38], this shift results from the filling of the conduction band. The Burstein–Moss shift is more pronounced in n-type GaAs than p-type material because of the lower density of states at the bottom of the conduction band. The spectral shape of the main emission peak becomes strongly asymmetric having a steep slope on the high

energy and smooth slope on the low energy side of the spectra. The asymmetry in the spectra of Fig. 1 at growth temperature > 600°C strongly indicates that indirect (without k-selection) B–B or B–A transitions dominate the emission across the gap. The FWHM of the B–B peak at 4.2 K of PL spectra increases with increasing growth temperatures. The electron concentration increases with increasing growth temperature on the GaAs substrates, as can be seen from the Fig. 2. But the relative increase in PL peak energy is higher on GaAs substrate than on Ge substrates. This shift may generally be attributed to possible thermal expansion mismatch and/or lattice mismatch. The possible tensile stresses resident in the film, may arise due to a large mismatch between the thermal expansions of GaAs and Ge. However, the thermal expansions of GaAs and Ge are very close to each other, i.e. 0.46 W cm^{-1}°C^{-1} and 0.6 W cm^{-1}°C^{-1}, respectively. This small difference cannot solely contribute to the shifts in PL peaks. Considering the lattice mismatch possibility, it is known that GaAs and Ge do exhibit a lattice mismatch of only 0.07% [39]. Such low magnitudes of lattice mismatch can not again be solely responsible for the shifts observed in PL peaks. Based upon these arguments, the observed shifts in the PL peak, in the present work, are mostly attributed to the increasing carrier concentration. The increase in PL peak shift towards higher energy corresponds to the increase in electron concentration. The electron concentrations measured by electrochemical capacitance voltage (ECV) profiler are
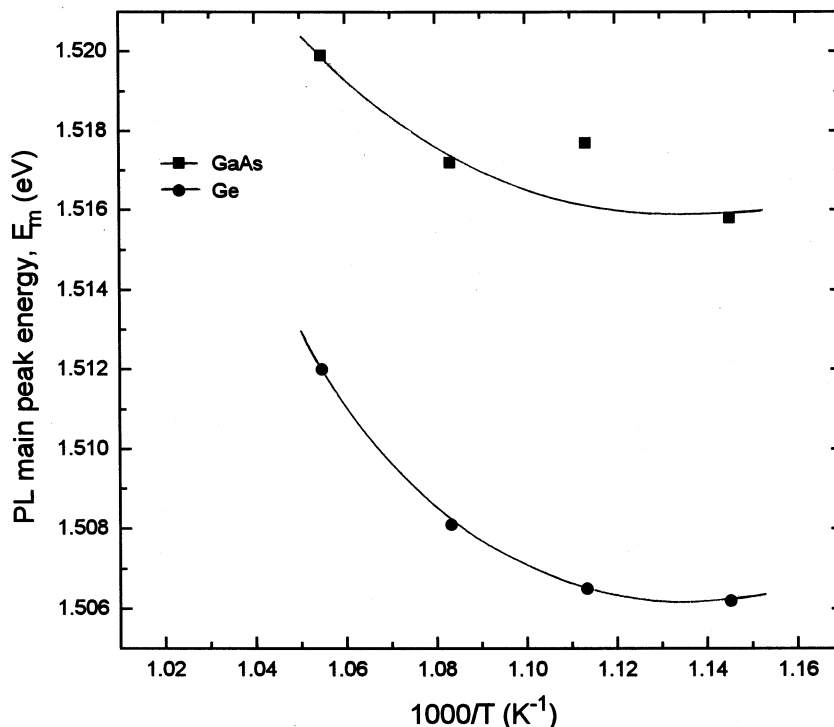
Fig. 4. PL peak energy as a function of growth temperature.

mentioned in both the figures for better understanding of the growth process on Ge substrates. These features can be explained by assuming that the Burstein–Moss phenomenon is effective in the present layers and that the Si doping efficiency in GaAs on GaAs substrate is higher than Si doping in GaAs on Ge substrates. A different level of Si incorporation in the GaAs on GaAs than Ge can be ruled out since the samples were grown at the same SiH_4 partial pressure. The role of Ge diffusion from the substrate into the epilayer is also ruled out because Ge diffusion into epilayer should increase the electron concentration. Masselink et al. [27] reported the first successful growth of GaAs and Al-GaAs/GaAs superlattices on (100) Ge substrates. They performed the PL measurements at 2 K on the Al-GaAs/GaAs superlattices and on the GaAs bulk layers grown on (100) Ge. In all cases, the luminescence intensity was comparable with that of similar structures grown on GaAs; this suggests that there were few (if any) additional nonradiative centers or deep traps in the case of bulk GaAs grown on (100) Ge and the dominant PL feature is a single peak whose maximum lies between 1.477 and 1.473 eV depending on the excitation intensity. This luminescence is due to the $e - Ge_{As}^0$ and $Ge_{Ga}^0 - Ge_{As}^0$ (free electron to acceptor and donor to acceptor) transitions involving Ge from the substrate, and has a phonon replica at 1.437 eV. This would indicate a Ge binding energy in GaAs of 43 meV. They also observed the luminescence from the recombination of bound excitons at 1.511 eV.

Prior to the growth of Si-doped GaAs on Ge, undoped GaAs on Ge (≈ 2 μm) was grown in order to check the Ge outdiffusion into the film. The PL spectrum of this film has only one peak at 1.5115 eV corresponding to the acceptor-bound exciton having FWHM of 10.3 meV and at 1.4749 eV corresponding to the phonon replicate of the acceptor bond exciton band. This PL spectrum suggests that there is no Ge outdiffusion from the substrate, but the Ge outdiffusion was observed by Fischer et al. [9] and Masselink et al. [27] in the MBE growth process. Timò et al. [15], however, observed a massive diffusion of Ge into epilayer by PL measurement in low growth rate (2 μm h$^-$ 1) of the MOCVD process. The difference in electron concentration on Ge and GaAs substrate could be the traps in the GaAs epilayer due to the defects originating from the heteroepitaxy. GaAs can be grown epitaxially on Ge in two equivalent orientations corresponding to an exchange of the Ga and As sublattices [40]. Domains of differing orientation are separated by an antiphase boundary (APB). Since GaAs is a polar material, the APBs have a net charge and are expected to act as scattering centers [40,41]. Antiphase boundaries in GaAs contain Ga–Ga and As–As bonds. Such bonds represent electrically charged defects, which may trap electrons [40]. This explanation becomes less likely at higher electron concentrations due to the requirement of very high trap concentrations. The lower electron concentration in GaAs on Ge substrate compared with GaAs substrate, may be due
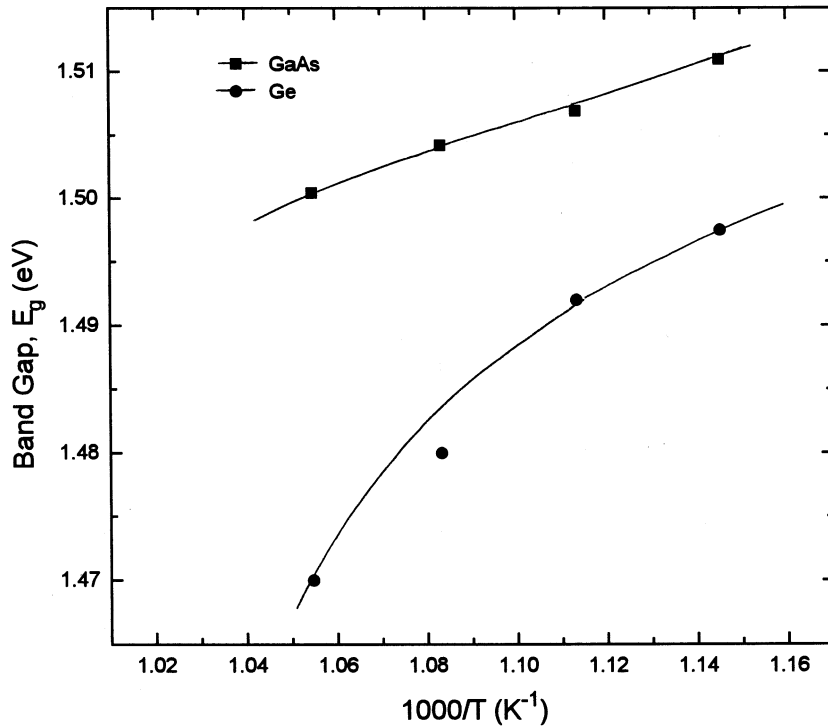
Fig. 5. Band gap vs. growth temperatures.

to the dislocation at the heterointerface, which tends to produce the gallium vacancies (V_{Ga}). This is a double acceptor and reduces the electron concentration on Ge substrate compared with GaAs substrates. This expla-

nation was less likely, because we did not observe any peak at around 1.2 eV corresponding to V_{Ga}-donor complex. Sieg et al [20] observed identical Si doping efficiencies on both GaAs and Ge substrates at doping
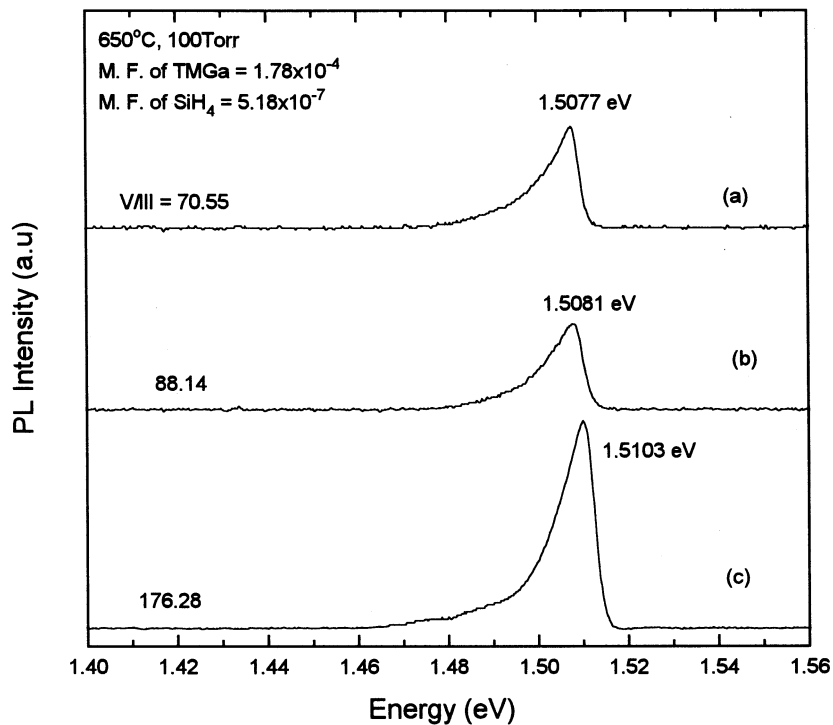
Fig. 6. 4.2 K PL spectra of Si-doped GaAs epilayers as a function of AsH$_3$ flow rate on Ge substrates. The corresponding electron concentrations are: (a) 1.8×10^{17} cm^{-3}, (b) 2.2×10^{17} cm^{-3}, (c) 2.54×10^{17} cm^{-3}.
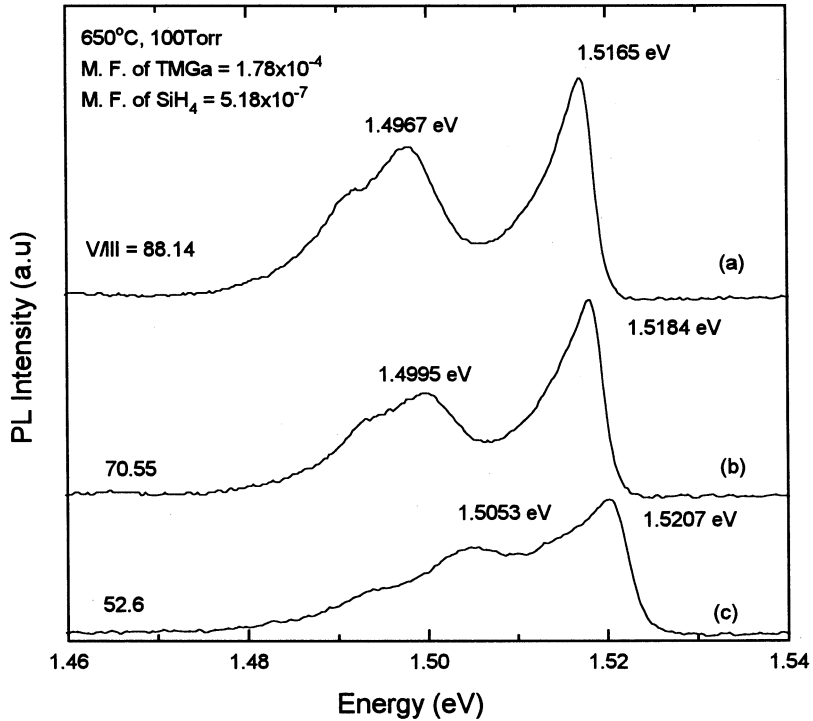
Fig. 7. 4.2 K PL spectra of Si-doped GaAs epilayers as a function of AsH$_3$ flow rate on GaAs substrates. The corresponding electron concentrations are: (a) 1×10^{17} cm^{-3}, (b) 2×10^{17} cm^{-3}, (c) 2.5×10^{17} cm^{-3}.

levels as low as 2.5×10^{15} cm^{-3}, grown by solid source MBE technique. In addition, they also suggested that for MBE films, Ge outdiffusion into the GaAs is an unlikely cause of the reduced apparent Si doping efficiency, since Ge usually produces n-type doping in GaAs.

The FWHM, $\Delta E(T)$ of the B–B peak at 4.2 K of PL spectra increases with increasing electron concentrations in both the cases (Fig. 3). The relative increase in FWHM is somewhat comparable for both Ge and
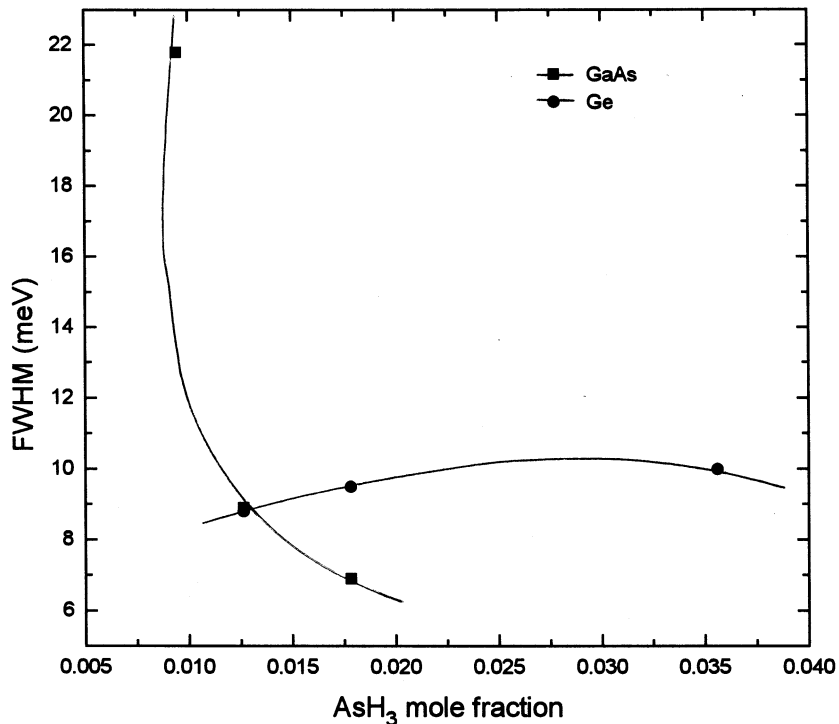
Fig. 8. FWHM of 4.2 K PL vs. AsH$_3$ mole fractions.
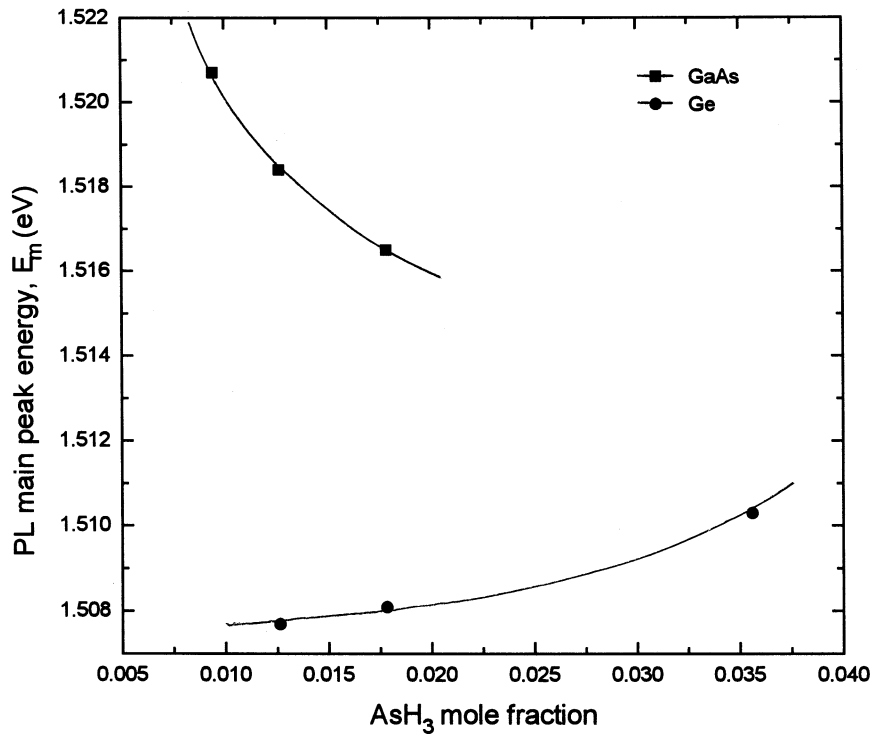
Fig. 9. PL peak energy vs. AsH$_3$ mole fractions.

GaAs substrates. The main peak energy shifted to higher energy as the growth temperature increased, i.e. as the electron concentration increased, which is primarily because of Burstein–Moss effect. Fig. 4 shows the PL peak energy with the growth temperatures in the range of 600–675°C. From this figure it is seen that the relative main PL peak position of Si-doped GaAs on GaAs substrate is higher than that of Si-doped GaAs on Ge substrate. The relative increase in peak position on GaAs than Ge substrates indicates the increase in
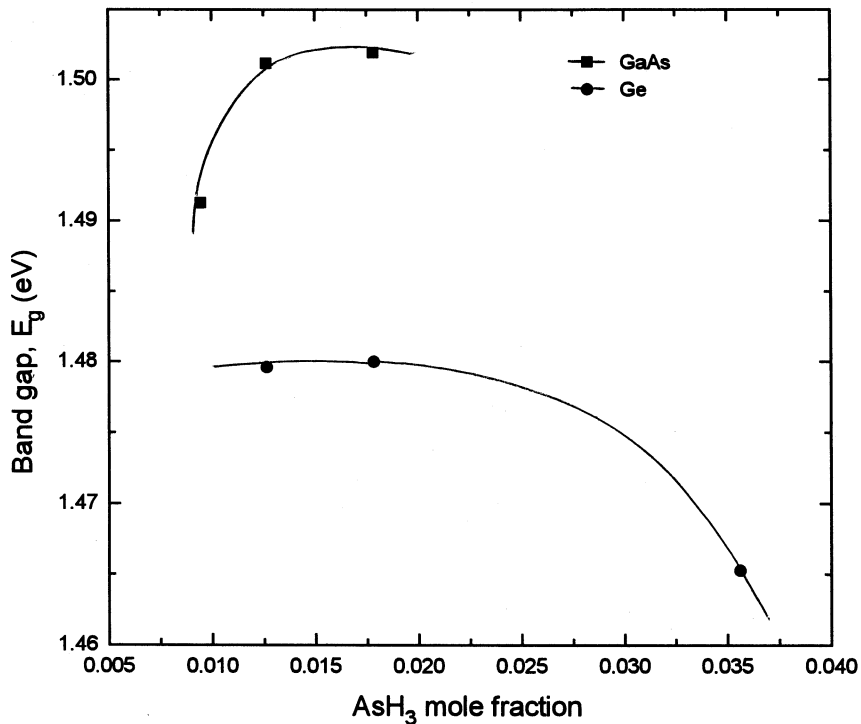
Fig. 10. Band gap vs. AsH$_3$ mole fractions.

650°C, 100 Torr
M. F. of AsH_3 = 1.57×10^{-2}
M. F. of SiH_4 = 5.18×10^{-7}

M. F. of TMGa = 8.88×10^{-5}

1.5081 eV

(a)

1.5081 eV

1.78×10^{-4}

(b)

1.5117 eV

2.68×10^{-4}

(c)

PL Intensity (a.u)

Energy (eV)
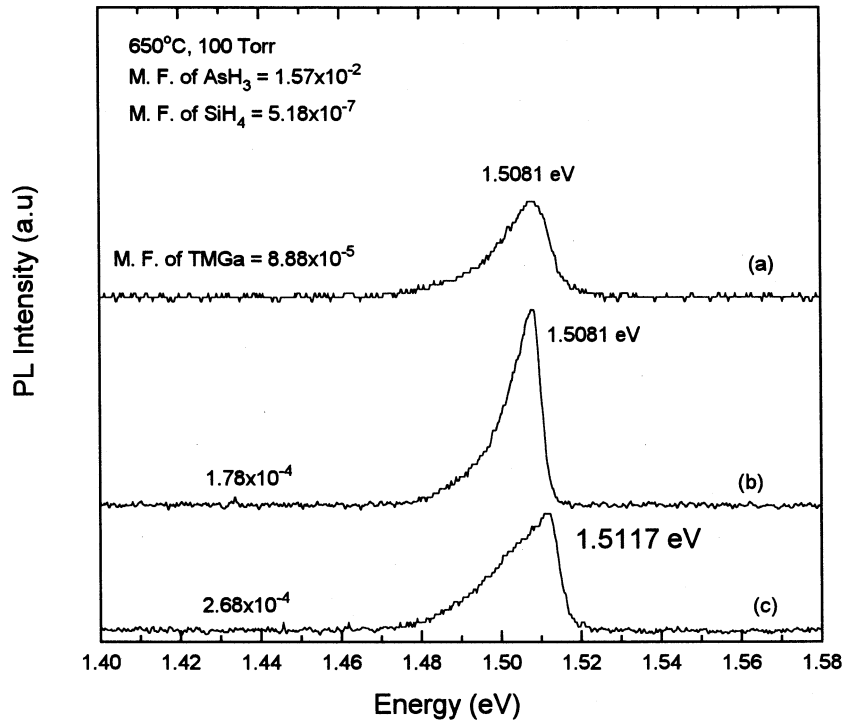
Fig. 11. 4.2 K PL spectra of Si-doped GaAs epilayers as a function of TMGa flow rate on Ge substrates. The corresponding electron concentrations are: (a) 1.96×10^{17} cm^{-3}, (b) 2.3×10 cm^{-3}, (c) 2.75×10 cm^{-3}.

carrier concentration on GaAs substrate than Ge substrate. It is very difficult to extract the exact band gap shift from the PL spectra because of life time broadening effect [42]. We determined the band gap, E_g of

doped GaAs, by a linear extrapolation to the energy axis, using a function of the type $f(E) = A(E - E_g)^{1/2}$, of the spectrum to the back ground level following the work by Olego and Cardona [42]. This method was also

650°C, 100 Torr
M. F. of AsH_3 = 1.57×10^{-2}
M. F. of SiH_4 = 5.18×10^{-7}

M. F. of TMGa
= 2.68×10^{-4}

1.5163 eV

1.4967 eV

(a)

1.4967 eV

1.5165 eV

1.78×10^{-4}

(b)

1.5206 eV

8.88×10^{-5}

(c)

PL Intensity (a.u.)

Energy (eV)
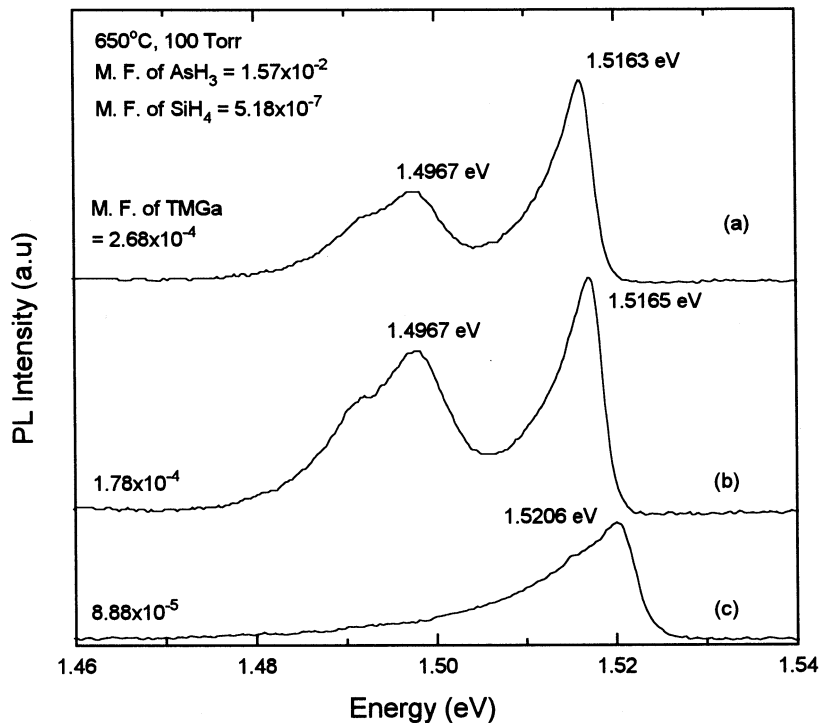
Fig. 12. 4.2 K PL spectra of Si-doped GaAs epilayers as a function of TMGa flow rate on GaAs substrates. The corresponding electron concentrations are: (a) 3.1×10^{17} cm^{-3}, (b) 3.64×10^{17} cm^{-3}, (c) 4×10^{17} cm^{-3}.
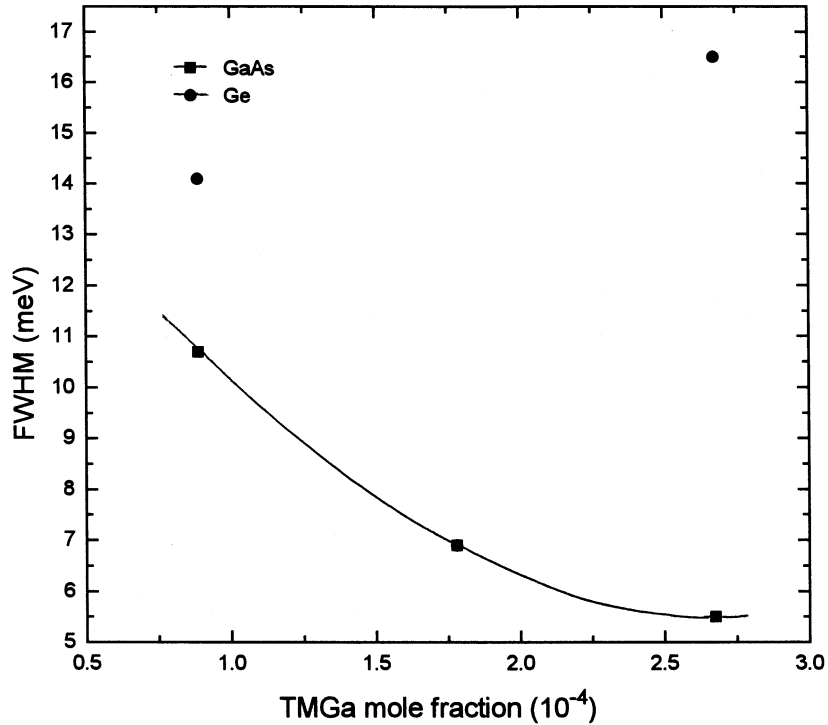
Fig. 13. FWHM of 4.2 K PL vs. TMGa mole fractions.

used by several authors for determination of E_g. Fig. 5 shows the band gap (measured at 4.2 K) versus the growth temperature of Si-doped GaAs on both GaAs and Ge substrates. The band gap decreases with the increasing growth temperature in both the cases, since the electron concentration increases with increasing growth temperature. The relative increase in band gap on GaAs substrate is higher than that of Ge substrate. Therefore, the Si incorporation efficiencies are different on both the polar and nonpolar substrates.
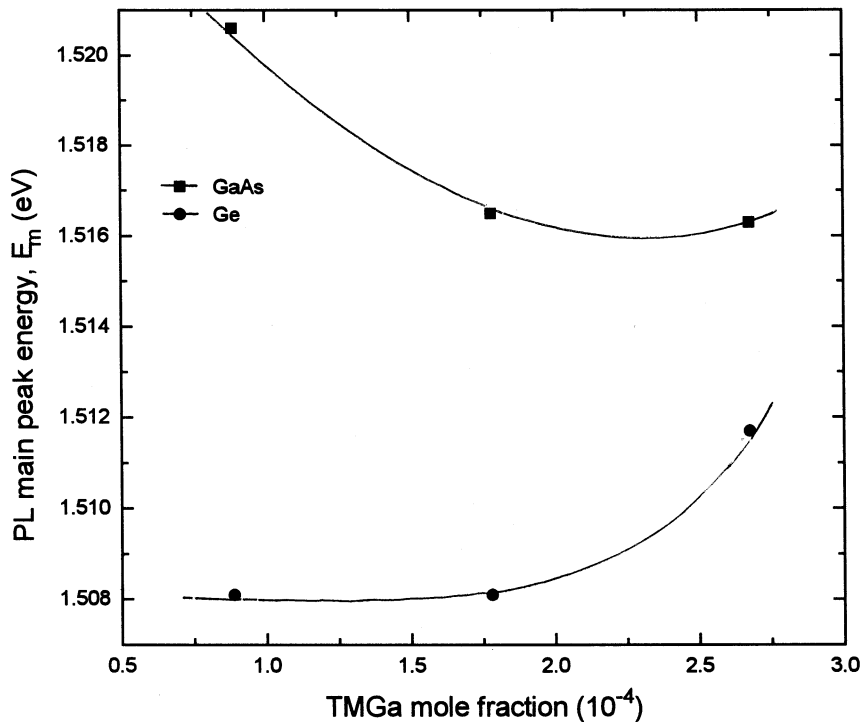
Fig. 14. PL peak energy vs. TMGa mole fractions.
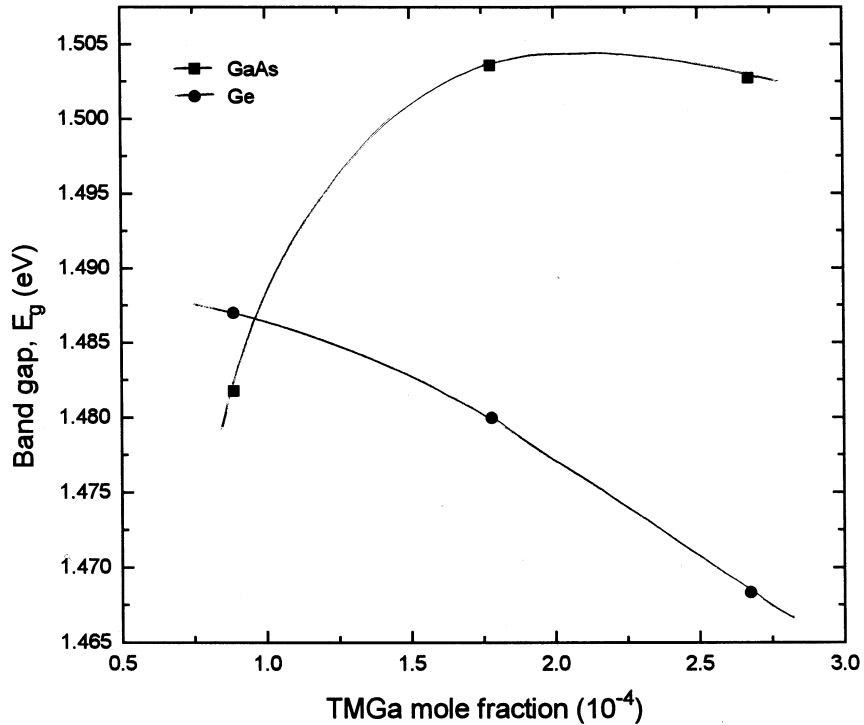
Fig. 15. Band gap vs. TMGa mole fractions.

3.2. Effect of AsH₃ variation on photoluminescence

To observe the effect of V/III ratio on the optical properties of Si-doped GaAs on Ge, the PL measurements were carried out at 4.2 K specifically on those samples grown at different AsH_3 flow rates. Fig. 6 shows the PL spectra of Si-doped GaAs for a fixed
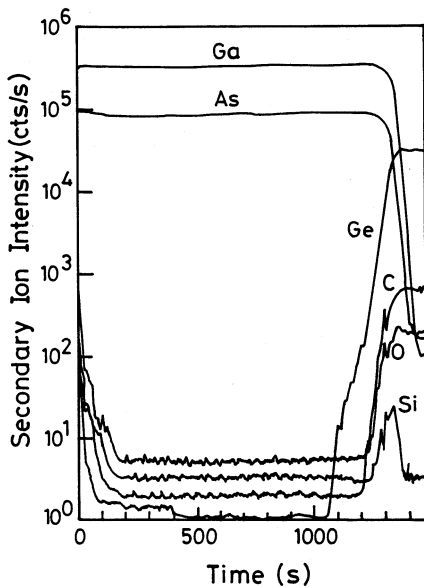
Fig. 16. SIMS depth profiles of compositional atoms around the heterointerface between the Si-doped GaAs epilayer and the Ge (100) substrate (sputtering rate ≈ 15 Å s⁻¹).

TMGa and SiH_4 mole fraction on Ge substrates. The three curves represent three different AsH_3 flow rates. It is seen from this figure that the PL main peak energy shifted to higher photon energies with increasing AsH_3 mole fractions. A vacancy-controlled model may be considered to explain such behavior. In the TMGa–AsH_3 system, the leading reaction to the formation of GaAs can be expressed as:

$$(CH_3)_3Ga + 3/2H_2 + V_{Ga} \overset{K_1}{\Leftrightarrow} Ga_{Ga} + 3CH_4 \qquad (1)$$

$$AsH_3 + V_{As} \overset{K_2}{\Leftrightarrow} As_{As} + 3/2H_2 \qquad (2)$$
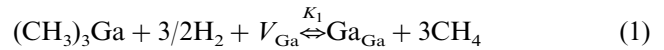
Where K_1 and K_2 are the equilibrium constants of the above reactions, then

$$\frac{[V_{Ga}]}{[V_{As}]} \equiv \frac{K_2}{K_1} \frac{P_{CH_4}^3}{P_{TMGa}} \frac{P_{AsH_3}}{P_{H_2}^3} \qquad (3)$$

Since Si as a donor is on the Ga sublattice, under equilibrium its incorporation should be proportional to the concentration of Ga vacancies, V_{Ga} [43]. The doping reaction is:

$$SiH_4 + V_{Ga} \overset{K_3}{\to} Si_{Ga} + 2H_2 \qquad (4)$$

From Eqs. (3) and (4) one can write,

$$\frac{[Si_{Ga}]}{[V_{As}]} \equiv \frac{K_2K_3}{K_1} \frac{P_{SiH_4}}{P_{TMGa}} \frac{P_{AsH_3}}{P_{H_2}^5} P_{CH_4}^3 \qquad (5)$$

An increase in P_{AsH_3} will increase gallium vacancy concentration, hence, the incorporation of Si on a Ga site is increased. The electron concentration is thus
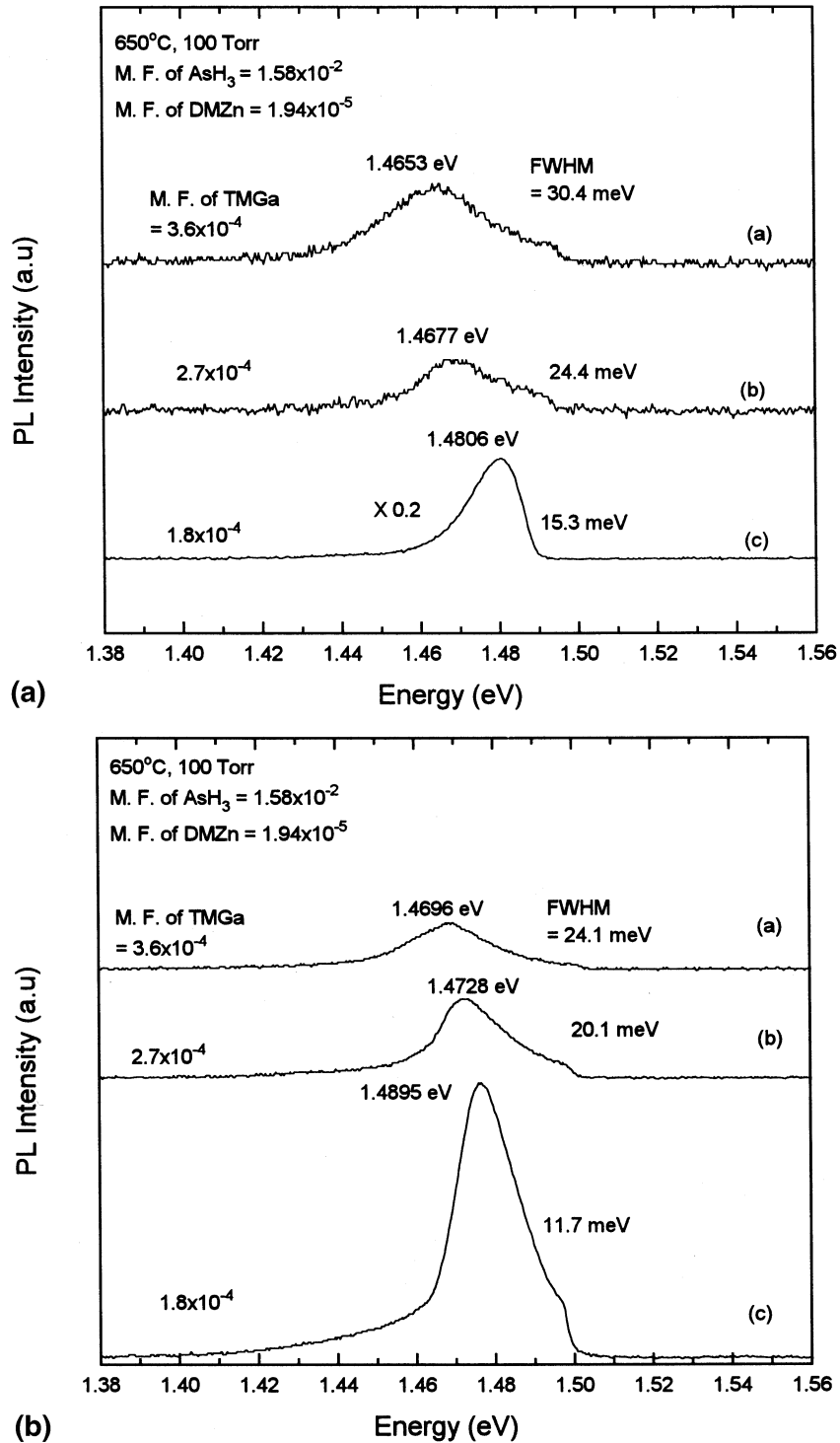
Fig. 17. (a) 4.2 K PL spectra of Zn-doped GaAs epilayers as a function of TMGa flow rate on Ge substrates. The corresponding hole concentrations are: (a) 6×10^{19} cm^{-3}, (b) 3.8×10^{19} cm^{-3}, (c) 3.5×10^{18} cm^{-3}. (b) 4.2 K PL spectra of Zn-doped GaAs epilayers as a function of TMGa flow rate on GaAs substrates. The corresponding hole concentrations are: (a) 2.5×10^{19} cm^{-3}, (b) 2.1×10^{19} cm^{-3}, (c) 1.5×10^{18} cm^{-3}.

increased when the AsH$_3$ mole fraction is increased and hence the PL main peak is shifted towards the higher energy with increasing AsH$_3$ mole fraction. According to Li et al. [13,14] the conditions for the suppression of

APDs are either the increase in higher V/III ratio or the lower growth rate (i.e. lower Ga flow). Since Ge diffuses into GaAs via Ga vacancies [15] and the Ga vacancy population will increase with increasing V/III

ratio and with decreasing growth rate, the Ge outdiffusion would be significant. This will be discussed in the TMGa variation case. There is some evidence in the literature that the cracked AsH_3 can roughen the Ge surface, leading to APDs and perhaps high dislocation densities. This may in turn produce high trap densities and less electron concentration [44]. However, we also studied the optical properties of low-doped layers with increasing AsH_3 mole fraction to check the possibility for an amphoteric effect of Si on GaAs substrate. Fig. 7 shows the PL spectra of Si-doped GaAs for a fixed TMGa and SiH_4 mole fraction on GaAs substrates. It is seen from this figure that the PL main peak energy shifted to lower photon energies since the electron concentration decreases with increasing AsH_3 mole fractions. The electron concentration decreases with the increasing V/III ratio for a given TMGa mole fraction and growth temperature of Si-doped GaAs on GaAs substrates, which is same as described by Bass [43]. According to the above model, as the AsH_3 concentration is increased, the V_{Ga} concentration increases, leading to a possible raise in the Si donor level. Conversely, as the AsH_3 concentration decreases, the As vacancies should increase and the Si as an acceptor should increase. The fact that the reverse behavior takes place suggests that the incorporation of Si is not controlled by the bulk thermodynamic properties of the lattice but by the surface kinetics process; the As appears to block the Si from the growing surface [43]. But we found that for a fixed concentration of SiH_4 mole fraction, the electron concentration decreases with increasing AsH_3 concentration on GaAs substrate. At the V/III ratio of 52.6, the growth induced point defects at 1.5053 eV called Künzel–Ploog defect exciton was observed similar to that observed in MBE-grown GaAs [45]. Even at this V/III ratio, the conduction band-to-acceptor (C–A) or donor-to-acceptor (D–A) transition was not observed, whereas it is frequently found in MOVPE grown GaAs. From these observations and from Hall mobility data, the lightly doped layers were not affected by the amphoteric nature of Si. On the other hand, the peak at 1.4967 eV and 1.4995 can influence the electrical properties of lightly doped layers. These peaks may be attributed to Zn and C (2S), respectively. The peak is asymmetric at lower AsH_3 mole fraction and becomes symmetric at higher AsH_3 mole fraction.

The FWHM of the B–B peak at 4.2 K of PL spectra increases with increasing AsH_3 mole fraction on Ge substrate and decreases with increasing AsH_3 mole fraction on GaAs substrates, as shown in the Fig. 8. From this figure it is seen that the FWHM decreases rapidly with AsH_3 mole fraction on GaAs substrates, whereas a slow increase in FWHM was observed on Ge substrates. The main peak energies shifted to higher energy as the AsH_3 mole fraction increased on Ge substrates as shown in Fig. 9 and the rapid decrease in

main peak energy was observed on GaAs substrate, since the carrier concentration decreases with increasing AsH_3 mole fraction on GaAs substrates. Fig. 9 shows the PL peak energy with the AsH_3 mole fractions on both the substrates. Fig. 10 shows the band gap versus the AsH_3 mole fraction of Si doped GaAs on both GaAs and Ge substrates. The band gap decreases with the increasing AsH_3 mole fraction on Ge substrate, since the carrier concentration increases with increasing AsH_3 mole fraction and increases on GaAs substrates. The relative increase in band gap on GaAs substrate is higher than that of Ge substrate. Therefore, the Si incorporation efficiencies with AsH_3 mole fraction are different on both the polar and nonpolar substrates.

3.3. Effect of TMGa variation on photoluminescence

To observe the effect of TMGa mole fraction on the optical properties of Si doped GaAs, the PL measurement were carried out at 4.2 K specifically on those samples grown at different TMGa flow rates. Fig. 11 shows the PL spectra of Si doped GaAs for a fixed AsH_3 and SiH_4 mole fraction on Ge substrates. The three curves represent three different TMGa flow rates. It is seen from this figure that the PL main peak energy shifted to higher photon energies with increasing TMGa mole fractions. However, a different observation was found in Si-doped GaAs on GaAs (100) substrate. In this case, the PL main peak energy shifted to higher photon energy with decreasing TMGa flow rates (Fig. 12), since the electron concentration decreases with increasing TMGa mole fractions. From Eq. (5) we found that the decrease in P_{TMGa} will increase in Ga-vacancy concentration. Since Si incorporates in Ga site and gives n-type, the electron concentration increases with decreasing TMGa flow rates and hence the PL peak energy shifted to higher photon energy. The possible explanation in the former case may be the increase in Ga interdiffusion in Ge with increasing TMGa, i.e. increasing growth rate and creates more Ga vacancy in the epitaxial film and hence Si incorporation increases.

The FWHM of the B–B peak at 4.2 K of PL spectra increases with increasing TMGa mole fraction on Ge substrates and decreases with increasing TMGa on GaAs substrates, as shown in the Fig. 13. From this figure it is observed that the FWHM decreases rapidly with TMGa mole fraction on GaAs substrates, whereas a slow increase in FWHM was observed on Ge substrates except at the TMGa mole fraction of 1.78×10^{-4}. The main peak energy shifted to higher energy as the TMGa mole fraction increased on Ge substrates as shown in Fig. 14. A rapid decrease in main peak energy was observed on GaAs substrate, since the carrier concentration decreases with increasing TMGa mole fraction on GaAs substrates. Fig. 14 shows the PL peak

energy with the TMGa mole fractions on both the substrates. Fig. 15 shows the band gap versus the TMGa mole fraction of Si doped GaAs on both GaAs and Ge substrates. The band gap decreases with the increasing TMGa mole fraction on Ge substrate, since the carrier concentration increases with increasing TMGa mole fraction. However, an increase in band gap was observed on GaAs substrates.

In order to check the interdiffusion of Ga into Ge, as well as the Ge outdiffusion into GaAs films, secondary ion mass spectroscopy (SIMS) technique was used. It is a powerful technique for quantitative measurements of dopant and impurity levels in semiconductors [46]. The concentration of particular element can be profiled through a layer using the dynamic SIMS technique. In this method, the mass spectral peak intensity corresponding to a particular ion is monitored as a function of time using a high sputtering rate. The results are presented in Fig. 16. The depth profiles (≈ 15 Å s^{-1}) of Ga, As, Ge, C, Si and O atoms in the Si-doped GaAs on Ge, measured by SIMS for a TMGa mole fraction of 1.78×10^{-4}. All atoms barely interdiffused at the heterointerface of the GaAs/Ge (100) substrate. The abrupt heterointerface in this film indicates the almost no outdiffusion of Ge into the GaAs epifilm [47].

3.4. Effect of TMGa variation on Zn-doped GaAs by photoluminescence

We have studied the Zn-doped p-type GaAs by PL spectroscopy on both Ge and GaAs substrates. In order to check the doping incorporation efficiencies of Si-doped and Zn-doped GaAs on both Ge and GaAs, we have carried out the Zn doping in GaAs. Fig. 17(a) and (b) show the PL spectra of Zn-doped GaAs on Ge and GaAs substrates, respectively. The hole concentration measured by ECV profiler are mentioned in both the figures for better understanding of the growth process on Ge substrates. The shift in main peak energy towards lower energy means the increase in hole concentrations. The hole concentration increases with increasing TMGa mole fractions and the main peak is shifted to lower energy with increasing TMGa mole fractions. This can be explained as, for a fixed growth temperature and mole fraction of DMZn, the hole concentration increases linearly with increasing growth rate. At high growth rates, the deposited zinc is absorbed into the epilayer before it can be evaporated from the surface. At lower growth rates, however, the residence time of Zn required for incorporation decreases, leading to increased Zn concentration via reduced Zn re-evaporation. From the Fig. 17(a), it is seen that the peak energy is less on Ge substrate compared with GaAs substrates. The PL main peak is shifted to lower energy with increasing TMGa mole fraction in both the cases. But the relative shift is more on Ge

substrates than GaAs substrates. It is also seen from these figures that the FWHM is also higher on Ge substrate than GaAs substrates and also the hole concentration. More systematic studies are felt necessary to explain such behavior, which are in progress.

4. Conclusions

Si-doped GaAs epitaxial layers grown by low pressure MOVPE on both Ge and GaAs have been investigated by PL spectroscopy as a function of growth temperature, AsH$_3$, and TMGa mole fraction. The B–B peak shifts to higher energy with increasing growth temperature, i.e. increasing electron concentrations due to Burstein–Moss shift. Band–acceptor transitions involving residual C acceptors are the dominant recombination processes at growth temperature below 600°C. Above 600°C, however, the dominating contribution to the spontaneous recombination process in n-type GaAs arises from (indirect) transitions between free electrons in the conduction band and localized acceptor-like centers in the deeper tail states above the valence band edge. The B–B peak also shifts to high energy as the AsH$_3$ and TMGa mole fractions increases on Ge substrates and shifts to lower energy when grown on GaAs substrates. A detailed comparative study of Si doping in GaAs on both Ge and GaAs substrate surfaces by low temperature PL spectroscopy has been investigated. The peak shift towards the higher energy side with increasing AsH$_3$ variation has been explained by vacancy controlled model The Zn doped GaAs data were presented on both Ge and GaAs for better understanding of the growth process.

References

[1] R.A. Metzger, Compound Semicond. 2 (6) (1996) 25.
[2] M. Kato, K. Mitsui, K. Mizugochi, N. Hayafuji, S. Ochi Y. Yukimoto, T. Murotan, K. Fujikawa, Proc. 18th IEEE Photovolt. Spec. Conf., 1985, p. 14.
[3] C. Flores, D. Passoni, G. Timd, in: Proc. European Space Power Conference, ESA SP-294, 1989, p. 507.
[4] C. Flores, B. Bollani, R. Campesato, F. Paletta, D. Passoni, G. Timò, A. Toson, Solar Energy Mater. 23 (1991) 356.
[5] K.I. Chang, Y.C.M. Yeh, P.A. Ilies, J.M. Tracy, R.K. Morris, Proc. 19th IEEE Photovolt. Spec. Conf., 1987, p. 273.
[6] P.A. Iles, Y.C.M. Yeh, F.H. Ho, C.L. Chu, C. Cheng, IEEE Electron Device Lett. 11 (1990) 140.
[7] N. Chand, J. Klem, H. Morkoç, Appl. Phys. Lett. 48 (1986) 484.
[8] S.C. Martin, L.M. Hitt, J.J. Rosenberg, IEEE Electron Device Lett. 10 (1989) 325.
[9] R. Fischer, W.T. Masselink, J. Klem, T. Henderson, T.C. McGlinn, M.V. Klein, H. Morkoç, J.H. Mazur, J. Washburn, J. Appl. Phys. 58 (1985) 374.
[10] A.G. Milnes, D.L. Feucht, Heterojunctions and Metal–Semiconductor Junctions, Academic, New York, 1972, p. 58.

[11] C. Flores, B. Bollani, R. Campensato, D. Passoni, G.L. Timò, Microelectron. Eng. 18 (1992) 175.

[12] S.J. Woitczuk, S.P. Tobin, C.J. Keavney, C. Bajgar, M.M. Sanfacon, L.M. Geoffroy, T.M. Dixon, S.M. Vernon, J.D. Scofield, D.S. Ruby, IEEE Trans. Electron Devices 37 (1990) 455.

[13] Y. Li, L. Lazzalini, L.J. Giling, G. Salviati, J. Appl. Phys. 76 (1994) 5748.

[14] Y. Li, G. Salviati, M.M.G. Bongers, L. Lazzarini, L. Nasi, L.J. Giling, J. Cryst. Growth 163 (1996) 195.

[15] G. Timò, C. Flores, B. Bollani, D. Passoni, C. Bocchi, P. Franzosi, L. Lazzarini, G. Salviati, J. Cryst. Growth 12 (1992) 440.

[16] S. Strite, D. Biswas, N.S. Kumar, M. Fradkin, H. Morkoç, Appl. Phys. Lett. 56 (1990) 244.

[17] P.R. Pukite, P.I. Cohen, J. Cryst. Growth 81 (1987) 214.

[18] K. Morizane, J. Cryst. Growth 38 (1977) 249.

[19] L. Lazzarini, Y. Li, P. Franzosi, L.J. Giling, L. Nasi, F. Longo, M. Urchulutegui, G. Salviati, Mater. Sci. Eng. B28 (1992) 502.

[20] R.M. Sieg, S.A. Ringel, S.M. Ting, E.A. Fitzgerald, J. Electron. Mater. (1997) (in press).

[21] K. Mizuguchi, N. Hayabuji, S. Ochi, T. Murotani, K. Fujikawa, J. Cryst. Growth 77 (1986) 509.

[22] T. Kawai, H. Yonezu, H. Yoshida, K. Pak, Appl. Phys. Lett. 61 (1992) 1216.

[23] T. Kawai, H. Yonezu, Y. Yamauchi, M. Lopez, K. Pak, J. Cryst. Growth 127 (1993) 107.

[24] N. Chand, J. Klem, T. Henderson, H. Morkoç, J. Appl. Phys. 59 (1986) 3601.

[25] R.L. Anderson, Solid State Electron. 5 (1962) 341.

[26] D.L. Miller, J.S. Harris Jr., J. Appl. Phys. Lett. 37 (1980) 1104.

[27] W.T. Masselink, R. Fischer, J. Klem, T. Henderson, P. Pearah, H. Morkoç, Appl. Phys. Lett. 45 (1984) 457.

[28] P.M. Petroff, A.C. Gossard, A. Savage, W. Wiegmann, J. Cryst. Growth 46 (1979) 172.

[29] J.M. Kuo, E.A. Fitzgerald, Y.H. Xie, P.J. Silverman, J. Vac. Sci. Technol. B11 (1993) 857.

[30] E.A. Fitzgerald, J.M. Kuo, Y.H. Xie, P.J. Silverman, Appl. Phys. Lett. 64 (1992) 733.

[31] Q. Xu, J.W.P. Hsu, E.A. Fitzgerald, J.M. Kuo, Y.H. Xie, P.J. Silverman, J. Eletron. Mater. 25 (1996) 1009.

[32] R. Fischer, H. Morkoç, D.A. Neuman, H. Zabel, C. Choi, N. Otsuka, M. Longerbone, L.P. Erickson, J. Appl. Phys. 60 (1986) 1640.

[33] G. Timò, L. Solevi, T.H. Nhung, Mater. Sci. Eng. B28 (1994) 474.

[34] G.L. Timò, C. Flores, Proc. 1st IEEE World Conf. Photovolt. Energy Conver., 1994, p. 2000.

[35] M.K. Hudait, P. Modak, S. Hardikar, S.B. Krupanidhi, Solid State Commun. 103 (1997) 411.

[36] V. Swaminathan, D.L. Van Haren, J.L. Zilko, P.Y. Lu, N.E. Schumaker, J. Appl. Phys. 57 (1985) 5349.

[37] D.J. Ashen, P.J. Dean, D.T.J. Hurle, J.B. Mullin, A.M. White, J. Phys. Chem. Solids 36 (1975) 1041.

[38] E. Burstein, Phys. Rev. 93 (1954) 632; T.S. Moss, Proc. Phys. Soc. Lond. B67 (1954) 775.

[39] S. Strite, M.S. Unlu, K Adomi, G.B. Gao, A. Aganval, A. Rockett, H. Morkoç, D. Li, Y. Nakamura, N. Otsuka, J. Vac. Sci. Technol. B8 (1990) 1131.

[40] H. Kroemer, J. Cryst. Growth 81 (1987) 193.

[41] P.M. Petroff, J. Vac. Sci. Technol. B4 (1986) 874.

[42] D. Olego, M. Cardona, Phys. Rev. B22 (1980) 886.

[43] S.J. Bass, J. Cryst. Growth 47 (1979) 613.

[44] N. Chand, F. Ren, A.T. Macrander, J.P. van der Ziel, A.M. Sergent, R. Hull, S.N.G. Chu, Y.K. Chen, D.V. Lang, J. Appl. Phys. 67 (1990) 2343.

[45] H. Kunzel, K Ploog, Appl. Phys. Lett. 37 (1980) 416.

[46] C.R. Brundle, C.A. Evans, S. Wilson, Encyclopedia of Materials Characterization, Butterworth-Heinemann, CT, 1992.

[47] M.K. Hudait, P. Modak, S. Hardikar, S.B. Krupanidhi, J. Appl. Phys. 83 (1998) 4454.